LATERAL DIFFUSION IN AN ARCHIPELAGO

The Effect of Mobile Obstacles

MICHAEL J. SAXTON

Plant Growth Laboratory, Department of Agronomy and Range Science, University of California, Davis, California 95616, and Laboratory of Chemical Biodynamics, Lawrence Berkeley Laboratory, University of California, Berkeley, California 94720

ABSTRACT Lateral diffusion of mobile proteins and lipids (tracers) in a membrane is hindered by the presence of proteins (obstacles) in the membrane. If the obstacles are immobile, their effect may be described by percolation theory, which states that the long-range diffusion constant of the tracers goes to zero when the area fraction of obstacles is greater than the percolation threshold. If the obstacles are themselves mobile, the diffusion constant of the tracers depends on the area fraction of obstacles and the relative jump rate of tracers and obstacles.

This paper presents Monte Carlo calculations of diffusion constants on square and triangular lattices as a function of the concentration of obstacles and the relative jump rate. The diffusion constant for particles of various sizes is also obtained. Calculated values of the concentration-dependent diffusion constant are compared with observed values for gramicidin and bacteriorhodopsin. The effect of the proteins as inert obstacles is significant, but other factors, such as protein–protein interactions and perturbation of lipid viscosity by proteins, are of comparable importance. Potential applications include the diffusion of proteins at high concentrations (such as rhodopsin in rod outer segments), the modulation of diffusion by release of membrane proteins from cytoskeletal attachment, and the diffusion of mobile redox carriers in mitochondria, chloroplasts, and endoplasmic reticulum.

INTRODUCTION

Many physiological processes involving cell membranes are thought to involve the lateral diffusion of mobile proteins and lipids within the membrane (Schlessinger, 1980; Axelrod, 1983; McCloskey and Poo, 1984). The diffusion of the mobile species of interest may be hindered by the presence of other species, and it would be useful to be able to evaluate quantitatively the effects of these obstacles on diffusion rates. This can be accomplished by treating lateral diffusion as a random walk on a two-dimensional lattice. The mobile species of interest (tracers) and the interfering species (obstacles) occupy sites on the lattice and undergo Brownian motion. The lipid is considered the solvent and not treated explicitly. The calculations are thus based on a lattice gas model of diffusion; this model takes into account only the hard-core repulsion of the particles.

This paper[1] presents Monte Carlo calculations of lattice diffusion of tracers in the presence of obstacles. In these calculations, each lattice point is occupied by an obstacle (at a concentration c), by a tracer (at a negligibly low concentration), or by a vacancy. Both tracers and obstacles are assumed to be mobile, but with different jump rates

---

[1]Preliminary results were presented at the 1986 Biophysical Society meeting (Saxton, 1986).

(Kutner and Kehr, 1983; Kehr and Binder, 1984). Tracers and obstacles carry out a random walk, jumping to adjacent vacant sites at the prescribed rates, and the mean square displacement of the tracers is obtained as a function of the number of time steps.

Let γ be the ratio of the jump rate of tracers to the jump rate of obstacles. Then two limiting cases are of particular interest.

(*a*) Percolation. If $\gamma \rightarrow \infty$, the obstacles are immobile. At low concentrations of obstacles, all vacancies are connected by some unbroken path and thus form an infinite cluster. A tracer can eventually diffuse to any vacant site on the lattice, so that as $t \rightarrow \infty$, the mean-square displacement $\langle r^2 \rangle \rightarrow \infty$ for all tracers. As the concentration of obstacles increases, isolated clusters of vacancies begin to appear. A tracer that starts on one of these finite clusters is trapped there, while tracers that start on the infinite cluster of vacancies can still diffuse to infinite $\langle r^2 \rangle$. At still higher concentrations of obstacles, only isolated clusters of vacancies are present. Each tracer is trapped on some cluster, and no long-range diffusion is possible. The percolation threshold c_p is defined as the highest concentration of obstacles at which an infinite cluster of vacancies exists. Long-range diffusion of tracers is allowed at area fractions of obstacles below c_p and is blocked at higher area fractions. For the square lattice, $c_p \sim 0.41$; for the triangular lattice, $c_p = 0.5$; and for the continuum, $c_p \sim 0.332$

(Stauffer, 1985; Saxton, 1982). This limit describes diffusion of lipid in the presence of immobile protein.

(*b*) Tracer diffusion. If $\gamma = 1$, obstacles and tracers move at the same rate, giving the concentration dependence of the lateral diffusion constant of a single species. This describes the diffusion of a protein at high concentration, such as rhodopsin in rod outer segments or proteins in mitochondria.

The distinction between these two limits is essential, and there has been some confusion on this point in the literature (Kell, 1984; Pink, 1985). If the obstacles are mobile, there is no percolation threshold, and long-range diffusion can occur at all concentrations, as shown by Pink (1985). But if the obstacles are immobile, there is a percolation threshold, and long-range diffusion is blocked when the area fraction of obstacles is greater than the percolation threshold. The key question is whether the obstacles are mobile or immobile on the time scale of the diffusion measurement.

This paper also discusses the variation in the tracer diffusion constant on a triangular lattice as the diffusing particles are changed from points to hexagons of increasing radius. These results show the geometrical dependence of the diffusion constant on particle size; the hydrodynamic dependence must be obtained from other treatments (e.g., Saffman and Delbrück, 1975; Galla et al., 1979).

GLOSSARY

a_i area of molecule of ith species
$A(R)$ number of lattice points in hexagon of radius R
c area fraction of obstacles (Eq. 10)
c_A area fraction of obstacles (Eq. 11)
c_p percolation threshold
D diffusion constant
D^* relative diffusion constant (Eq. 2)
γ ratio of jump rate of tracers to jump rate of obstacles
ℓ lattice spacing
$\langle r^2 \rangle$ mean-square displacement
R radius of hexagon in units of ℓ

METHODS

The Monte Carlo calculations (Kutner and Kehr, 1983) are carried out for square or triangular lattices. Initially, obstacles and tracers are distributed randomly on the lattice at the required concentrations. Then both species are allowed to move to adjacent unoccupied sites by a random walk at the prescribed jump rates. A move by an obstacle can be blocked by another obstacle or by a tracer. A move by a tracer can be blocked by an obstacle, but not by another tracer. Tracers can occupy the same vacancy; the only interaction among tracers is through their effect on the motion of obstacles. Except for this interaction, the tracers form an ensemble of particles diffusing independently through the same set of obstacles. The mean-square displacement of the tracers is obtained as a function of time, and the diffusion constant is obtained from a least-squares fit to the equation

$$\langle r^2(t) \rangle = 4Dt + A + B \ln t. \tag{1}$$

The terms $A + B \ln t$ come from the long-time tail in the two-dimensional velocity autocorrelation function (Van Beijeren and Kutner, 1985; Tahir-Kheli and El-Meshad, 1985). Their effect is usually small: typically they change the diffusion constant by 1–2%. At high concentrations, the effect is greater, and they lower the diffusion constant by up to 25%.

The initial positions of the tracers are random, so that in calculations with immobile obstacles the tracers may be on finite or infinite clusters of vacancies. The diffusion constant is changed if the tracers are placed only on infinite clusters (Stauffer, 1985).

The algorithm used is as follows. At each time step, a random number is used to decide whether to move a tracer or an obstacle. When an obstacle is to be moved, another random number is used to choose which obstacle is to be moved. When a tracer is to be moved, all tracers are moved, but the move for each tracer is chosen independently. In each move, the particle—obstacle or tracer—attempts to move to a randomly chosen nearest-neighbor site. If the site is vacant, the particle moves to that site; if the site is blocked, the particle remains in place. Pseudorandom numbers are generated by a Tausworthe shift register sequence (Kirkpatrick and Stoll, 1981; Kalle and Wansleben, 1984).

For the calculations with $\gamma = 1$, the algorithm is much simpler. All particles move with the same jump rate; there is no need to distinguish tracers and obstacles. All the particles carry out a random walk, and their mean-square displacements are obtained as a function of time.

For diffusion of hexagons at low densities, the initial positions of the particles are simply chosen at random. The highest density that can be obtained by random filling is called the random parking limit (Onoda and Liniger, 1986, and references cited therein). At densities above this limit, a more complicated procedure is required to obtain the initial configuration. The lattice is filled at close packing, and overlaps at the edges due to periodic boundary conditions are eliminated by random deletion of overlapping hexagons. Then hexagons are eliminated randomly to yield the required concentration. A random walk is carried out for a fixed time to randomize the starting configuration. Then the positions of the particles are recorded, and the random walk is continued to give the mean-square displacements as a function of time.

The lattice size was 201×201, 256×256, or 256×512, with periodic boundary conditions. Typically, for $\gamma \neq 1$, 200 tracers were used, and 25 different initial distributions of particles. Increasing the number of initial distributions and decreasing the number of tracers had little effect on the results. For point tracers with immobile point obstacles at an area fraction $c = 0.3$ on the square lattice, the relative diffusion constant (Eq. 2) is $D^* = 0.2592 \pm 0.0031$ (mean $\pm$ SD) for four runs with values ranging from 200 tracers with 25 different initial distributions to 25 tracers with 200 initial distributions.

The length of the runs ranged from 0.13 to 20.0 million time steps, depending on the densities of particles and the relative jump rates. The length of the run can be expressed in Monte Carlo steps per particle (MCS/p): the total number of attempted moves per mobile particle. For percolation on the square lattice, 0.13 million MCS/p were used; for the calculations with mobile obstacles on the square lattice, 100–1,700 MCS/p; and for tracer diffusion of hexagons, 40–1,600 MCS/p, with typical values of 200–400. The lower values were for high concentrations of particles, when the computer time needed was large.

Tests were made varying the seed of the random number generator. For tracer diffusion of point particles on the square lattice at $c = 0.3$, and 173 MCS/p, the relative diffusion constant D^* was 0.5776 ± 0.0010 (mean $\pm$ SD) for four runs, and a run to 692 MCS/p (8.3 million time steps) gave $D^* = 0.5780$.

Extensive Monte Carlo calculations of tracer diffusion of point particles on a square lattice were published by Tahir-Kheli and El-Meshad (1985) and by Van Beijeren and Kutner (1985). All but one of my diffusion constants differed from theirs by 0.4% or less, within the published error estimates. At one concentration of obstacles, my value of D^* differed from theirs by 3.1%.

RESULTS AND DISCUSSION

Effect of Obstacles

The Monte Carlo calculations give the mean-square displacement $\langle r^2 \rangle$ of the tracer as a function of time. The slope of this line at large times is proportional to the

990

diffusion constant (Eq. 1). Define a relative diffusion constant

$$D^*(c) = D(c)/D(0),\qquad(2)$$

where $D(c)$ is the diffusion constant of the tracer at a concentration c of obstacles, and $D(0)$ is the diffusion constant of the tracer in the absence of obstacles. In two dimensions

$$D(0) = \ell^2\Gamma/4,\qquad(3)$$

where ℓ is the lattice spacing and Γ is the jump frequency. The concentration c is an area fraction, defined as the ratio of the number of lattice points occupied by obstacles to the total number of lattice points.

Suppose that the obstacles are immobile. As shown in Fig. 1 a, when the area fraction of point obstacles is below the percolation threshold c_p, at large times $\langle r^2\rangle$ increases linearly with time, with a slope $4D$. As the area fraction c of obstacles increases, the diffusion constant decreases. When the area fraction of immobile obstacles is above c_p,
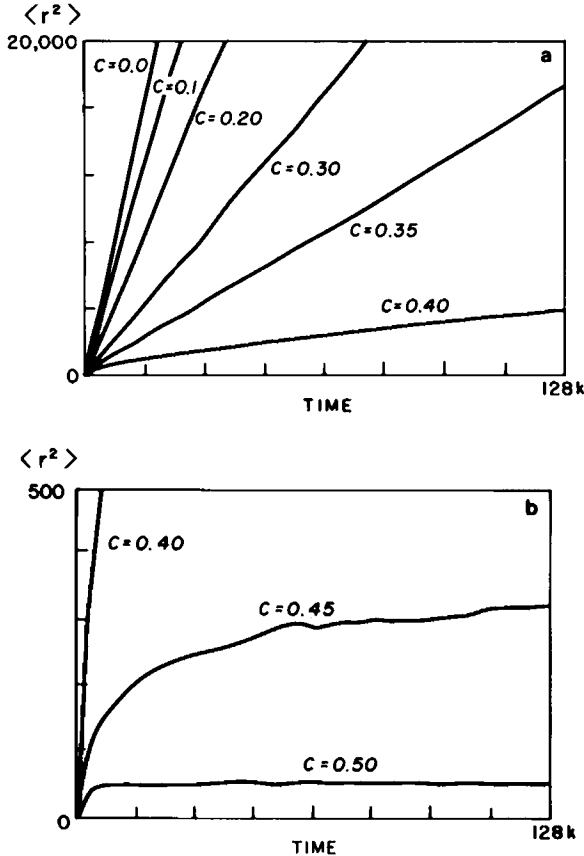

FIGURE 1 Mean-square displacement $\langle r^2\rangle$ of point tracers as a function of time, for percolation on the square lattice with various area fractions c of immobile point obstacles. The diffusion constants $D(c)$ are one-fourth of the limiting slopes of these lines as $t \to \infty$. (a) Area fractions of obstacles below the percolation threshold $c_p \sim 0.41$. (b) Area fractions of obstacles near and above the percolation threshold. Note the change in vertical scale. The unit of length is the lattice spacing, and the unit of time is the reciprocal of the jump frequency. (1k = 1,024).

no long-range diffusion is possible. Tracers are isolated on finite clusters, and as $t \to \infty$, $\langle r^2\rangle$ approaches a finite limit, as shown in Fig. 1 b. This limit is proportional to the average radius of gyration of the finite clusters (Straley, 1980; Mitescu and Roussenq, 1983).

Thus, if the obstacles are immobile, the long-range diffusion constant of the mobile species goes to zero when the area fraction of obstacles reaches the percolation threshold, as shown in Fig. 2. The value of c_p is from Gebele (1984) and was obtained by methods distinct from those used here.

When the obstacles are mobile, long-range diffusion can occur at all concentrations of obstacles, but the diffusion constant is a function of both c and the relative jump rate γ. A theoretical expression for $D^*(c, \gamma)$ was obtained by Tahir-Kheli (1983) and by Van Beijeren and Kutner (1985). Van Beijeren and Kutner considered the correlations between the tracer and the special vacancy, defined as the vacancy with which the tracer exhanges positions at $t = 0$. Both the tracer and the special vacancy are assumed to move in a continuous-time random walk, but with different jump rates. The diffusion constant can be expressed in terms of the correlation factor $f(c, \gamma)$:

$$D^*(c, \gamma) = (1 - c)f(c, \gamma).\qquad(4)$$

They obtain

$$f(c, \gamma) = \frac{\{[(1 - \gamma)(1 - c)f_o + c]^2 + 4\gamma(1 - c)f_o^2\}^{1/2} - [(1 - \gamma)(1 - c)f_o + c]}{2\gamma(1 - c)f_o},\qquad(5)$$

where

$$f_o = [1 - \alpha]/[1 + (2\gamma - 1)\alpha],\qquad(6)$$

where c is concentration of obstacles, γ is jump rate of tracers/jump rate of obstacles, and α is a constant equal to $1 - 2/\pi$ for the square lattice, 0.2820 for the triangular lattice, and 0.5000 for the honeycomb lattice (Le Claire, 1970). (Here $\alpha = (1 - f)/(1 + f)$, where f is given in Le
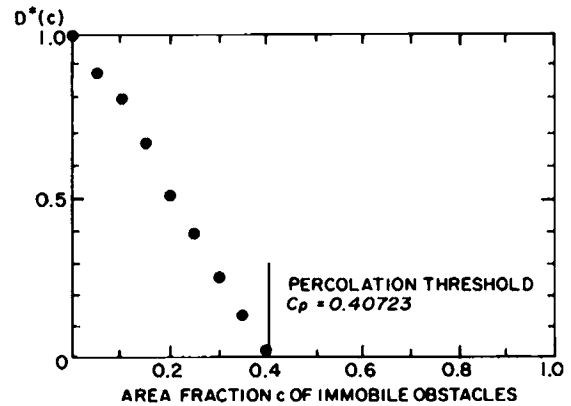
FIGURE 2 Diffusion constant $D^*(c)$ of point tracers as a function of area fraction c of point immobile obstacles on the square lattice.

Claire's Table I. Note that α is equivalent to $-\langle\cos\theta\rangle$ in the literature of solid-state diffusion.) From Eq. 3, the ratio of jump rates can be obtained from the observed diffusion constants at low concentrations of obstacles:

$$\gamma = D_{\text{tracer}} (c = 0)/D_{\text{obstacle}} (c = 0). \qquad (7)$$

In Fig. 3, values of D^* for the square lattice are shown as a function of c for various values of γ. Theory (Eqs. 4–6) and Monte Carlo results agree well, with two exceptions.

(a) The theory does not predict the percolation limit or the $D^*(c)$ curve for $\gamma \rightarrow \infty$ correctly. The theory gives a percolation threshold 10–15% too low. This is a general problem of mean-field theories: they do not include enough higher correlations to predict the percolation threshold accurately. The theoretical curve for $\gamma = 10$ shows the same problem to a lesser extent.

(b) The discrepancies at high values of c are due to the limited length of my Monte Carlo runs.

For $\gamma = 0.1, 0.33$, and 3.33, the average deviation of the Monte Carlo values of D^* from theory is 5%, and the largest deviation is 10%. For $\gamma = 1.0$, the average deviation is 1.2%, and the largest deviation is 4.6%.

In Fig. 3, note the large increase in D^* if γ is changed from ∞ (immobile obstacles) to 1 (mobile obstacles) at a fixed area fraction of obstacles. At $c = 0.3$, below the percolation threshold, D^* increases from 0.27 to 0.58, while at $c = 0.5$, above the percolation threshold, D^* is zero for immobile obstacles, and 0.36 when $\gamma = 1$. Thus, the release of proteins from cytoskeletal attachment could modulate the diffusion rates of all mobile species, lipid and protein, in the membrane. This has been observed in blebs (Webb et al., 1981; Tank et al., 1982b), bulbous lymphocytes (Wu et al., 1982), and spherocytes (Koppel et al., 1981b). To describe these results in terms of the Monte Carlo model, one would need to calculate the diffusion constant of point tracers in the presence of mobile hexagonal obstacles.
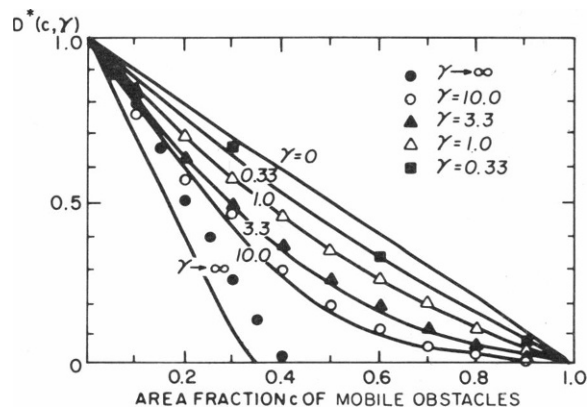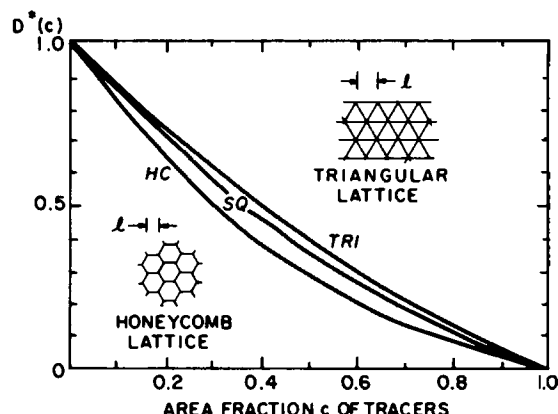

FIGURE 4 Tracer diffusion constant ($\gamma = 1$) as a function of area fraction from Eqs. 4–6 for various two-dimensional lattices: square, triangular, and honeycomb. The triangular and honeycomb lattices are shown in the insets; the lattice spacing is ℓ.

A very simple case shown in Fig. 3 is the limit $\gamma = 0$. Then the positions of the obstacles change so quickly that there is no correlation between successive tracer jumps. A fraction c of the tracer jumps is blocked; the remaining fraction $1 - c$ is successful. The only effect of the obstacles is to lower the effective jump rate of the tracers by a factor of $1 - c$, so that $D^* = 1 - c$.

According to theory (Van Beijeren and Kutner, 1985), the tracer diffusion constant is not particularly sensitive to the lattice structure, as shown in Fig. 4 for the triangular lattice (coordination number $z = 6$), the square lattice ($z = 4$), and the honeycomb lattice ($z = 3$).

Effect of the Radius of the Diffusing Particle

The calculations presented so far assume point tracers and obstacles on a lattice. If the calculations are to be applied to protein diffusion, the effect of the size of the protein on the diffusion constant must be considered. The hydrodynamic dependence of the diffusion constant on protein radius can be treated by a continuum diffusion model (Saffman and Delbrück, 1975; Hughes et al., 1982) or by a free volume model (Galla et al., 1979; MacCarthy and Kozak, 1982) as appropriate (Vaz et al., 1984; Clegg and Vaz, 1985). There is also a geometrical size dependence, which can be examined by Monte Carlo calculations.

We assume that the observed diffusion constant at a protein concentration c is

$$D_{\text{obs}}(c) = D_{\text{obs}}(0)D^*(c), \qquad (8)$$

where $D_{\text{obs}}(0)$ is the observed diffusion constant at low protein concentration. This equation follows directly from Eq. 2 on replacing $D(0)$ and $D(c)$ with the experimental values. The approximation implicit in this equation is that the hydrodynamic size dependence is contained entirely in $D_{\text{obs}}(0)$, and the geometric concentration dependence is contained entirely in $D^*(c)$, which accounts for the hard-

FIGURE 3 Diffusion constant $D^*(c, \gamma)$ for point tracers on a square lattice as a function of c, the area fraction of point obstacles, and γ, the ratio of tracer jump rate to obstacle jump rate. The lines are from theory (Eqs. 4–6), and the points are from the Monte Carlo calculations.

core repulsion of the proteins. In reality, $D^*(c)$ will be perturbed by additional protein–protein interactions, and the hydrodynamic size dependence will vary with concentration. But the approximation in Eq. 8 ought to capture the essential physics.

For hexagonal tracers, the area fraction c is defined as the fraction of lattice points within, or on the perimeter of, a hexagon. Define the radius R of a hexagon as the distance (in lattice spacings) from the center to a vertex. Then the number of lattice points in the hexagon is

$$A(R) = 3R^2 + 3R + 1. \qquad (9)$$

A lipid corresponds to a single lattice point, with $R_L = 0$, $A_L = 1$, and a protein corresponds to a hexagon of appropriate radius R. In a mixture of lipids of area a_L per molecule and proteins of area a_P per molecule, the value of R can be found by setting the ratio a_P/a_L equal to A_P/A_L, and solving Eq. 9 for R.

If the number of hexagons is N_H and the total number of lattice points is N_S, then

$$c = A(R)N_H/N_S. \qquad (10)$$

This corresponds to f_A of Pink (1985) and f_{LP} of Eisinger et al. (1986). One could also define an area fraction c_A in terms of the areas of the hexagons, giving

$$c_A = 3R^2 N_H/N_S, \qquad (11)$$

equivalent to f of Eisinger et al. (1986). With the definition Eq. 10, the entire space is occupied with either lipid or protein; with the definition Eq. 11, it is not (Eisinger et al., 1986). We therefore use Eq. 10.

No overlap of hexagons is allowed, even at edges or vertices, as in Pink (1985). Eisinger et al (1986) allow obstacles to overlap at edges and vertices.

The concentration dependence of the tracer diffusion constant for various radii between 0 to 16 is shown in Fig. 5. There is a large change in $D^*(c)$ on going from $R =$

0 to $R = 1$, but for $R = 1$–4, the values of $D^*(c)$ are very weakly dependent on R. For practical purposes this R-dependence can be ignored; a least-squares fit to the Monte Carlo values gives

$$D^*(c) = 1 - 2.1187c + 1.8025c^2$$
$$- 1.6304c^3 + 0.9466c^4, \qquad (12)$$

good to $\pm 5\%$ or better for $c \leq 0.65$, $R = 1$–4. Here c is defined by Eq. 10; if Eq. 11 were used, there would be a strong dependence on R. Eisinger et al. (1986) found a similar sensitivity to the definition of area fraction chosen.

If we identify each lattice site with one lipid molecule and assume a lattice constant of 0.8 nm, as in Eisinger et al. (1986), the area per lipid is 0.554 nm². If we then assume that the hexagons correspond to proteins of thickness 4.0 nm and density 1 g/cm³, and use Eq. 9, we find that hexagons of radius 1–4 correspond to proteins of mass 10–80 kD. (Pink [1985] identifies each lattice site with one hydrocarbon chain and assumes a lattice constant of 0.6 nm, so that a hexagon of radius 4 corresponds to a protein of mass 45 kD.)

Values of D^* for $R = 8$ and $R = 16$ are slightly higher than those for $R = 1$–4 at the same area fraction. When the area fraction c is constant, the total number of occupied lattice sites is constant. As R increases, these occupied sites are grouped into fewer, larger hexagons, which interfere with one another less. In the limit of very large R, all the occupied sites are included in a single large hexagon, for which D^* is one. A similar observation was made by Eisinger et al. (1986) in their studies of the diffusion of point tracers in the presence of immobile hexagonal obstacles of radius 1–3. (For radius zero, their model is simply percolation on a triangular lattice; results for this case were published by Li and Strieder [1982].)

In the plots of $D^*(c)$ for $R = 1, 2, 4, 8,$ and 16, there is no discontinuity in slope such as Pink (1985) reported for $R = 4$. Not enough values were calculated for $R = 3$ to show whether there is a discontinuity. Pink's values are a few percent lower than those obtained here.

Applications

Several measurements have been made of the lateral diffusion constants of proteins and lipids as a function of protein concentration (Schindler et al., 1980; Tank et al., 1982a; Peters and Cherry, 1982; Chazotte et al., 1984; Sowers and Hackenbrock, 1985). The concentration dependence will be influenced by factors other than obstruction: for example, direct or indirect protein–protein interactions, or interactions with the cytoskeleton. The Monte Carlo calculations will enable us to separate the purely geometrical percolation effects—that is, the effects of the hard-core repulsion—from the effects of other interactions.

Evaluation of the area fraction of obstacles requires attention to protein structure. Consider an integral protein
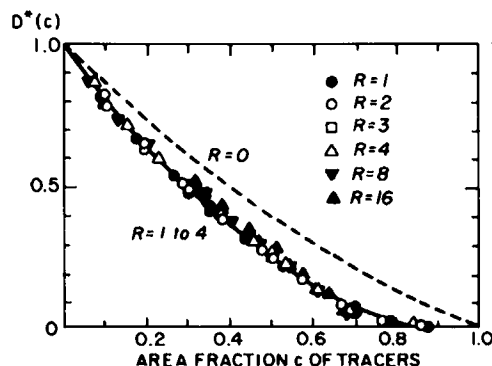

FIGURE 5 Tracer diffusion constant $D^*(c)$ as a function of the area fraction c of tracers for points $(R = 0)$ and hexagons of radius $R = 1$–16 on the triangular lattice. Dashed line, theoretical curve for $R = 0$ from Eqs. 4–6. Solid line, least-squares fit for $R = 1$–4 from Eq. 12. Points, values of $D^*(c)$ from Monte Carlo calculations.

with a wide hydrophilic region and a narrow hydrophobic region. A small hydrophobic molecule like ubiquinone will see only the hydrophobic region, while a large integral protein will interact with both regions. The relevant radius of the obstacle will thus be different, and the appropriate area fraction of obstacles will be different.

Peters and Cherry (1982) have measured the diffusion constants of bacteriorhodopsin (BR) and the lipid analogue dioctadecyloxacarbocyanine (diO-C_{18}[3]) as a function of BR concentration in multibilayers of dimyristoylphosphatidylcholine (DMPC). Tank et al. (1982a) have made similar measurements on gramicidin (GR) and the lipid analogue N-4-nitrobenzo-2-diazole phosphatidylethanolamine (NBD-PE).

Protein Diffusion. The area fraction of protein is calculated from the relation

$$c = \frac{1}{1 + \frac{a_L \, n_L}{a_P \, n_P}}, \quad (13)$$

where a_L is the area of a lipid molecule, a_P is the area of a protein molecule, and n_L/n_P is the molar ratio of lipid to protein. For DMPC, $a_L = 0.657$ nm^2 (Lewis and Engelman, 1983), for BR, $a_P = 8.75$ nm^2 (Henderson and Unwin, 1975), and for GR, $a_P = 1.13$ nm^2 (Tank et al., 1982a). From Eq. 9, BR corresponds to a hexagon of radius 1.59, and GR corresponds to a hexagon of radius 0.20. $D_{BR}{}^*$ can therefore be obtained from Eq. 12, and $D_{GR}{}^*$ is approximately the value from Eqs. 4–6 for $\gamma = 1$.

To interpret these experiments, we also need the diffusion constants at infinite dilution, $D_{obs}(0)$. These could be obtained by using Eqs. 4–6 or 12 to extrapolate the measured value at the lowest concentration to zero concentration. Here it is more convenient to show the calculated and observed values on log–log plots, so that the choice of $D_{obs}(0)$ simply corresponds to a vertical shift of the calculated curve.

Results are shown in Fig. 6. The calculated values from Eqs. 4–6 and Eq. 12 are shown in Fig. 6 *a*; observed values for BR and GR, in Fig. 6 *b*. Clearly the observed values of D fall off more sharply at high concentrations than the calculations predict.

Similar results are obtained for rhodopsin. The diffusion constant of rhodopsin in rod outer segments (ROS) is given by Poo and Cone (1974) and by Liebman and Entine (1974). No value for the diffusion constant in ROS lipids at low protein concentration is available, but Vaz et al. (1982) measured D for bovine rhodopsin at low concentrations in DMPC multibilayers. In Eq. 2 we use the diffusion constants obtained by Poo and Cone (1974) and Liebman and Entine (1974) for $D(c)$, and the results of Vaz et al. (1982) for $D(0)$. We find that $D_{obs}^* \sim 0.3$–0.4. According to Dratz and Hargreave (1983), $c = 0.24$ in ROS, so from Eq. 12, $D^* \sim 0.6$.
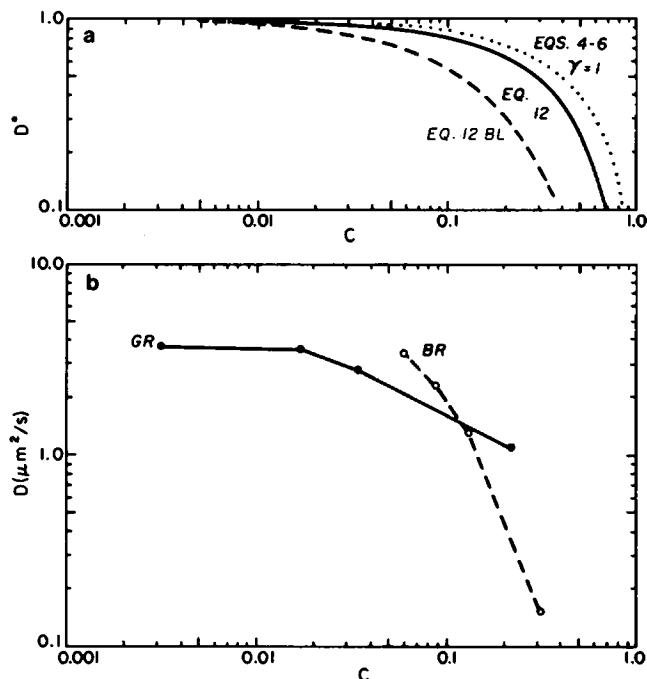

FIGURE 6 Lateral diffusion constants for proteins as a function of the area fraction of protein. (*a*) Calculated values for $R = 0$ from Eqs. 4–6 (*dotted line*) and $R = 1$–4 from Eq. 12. The dashed curve is calculated from Eq. 12 assuming 30 boundary lipids rigidly attached to BR. (*b*) Observed values for bacteriorhodopsin in DMPC (from Table 3 of Peters and Cherry, 1982) and gramicidin in DMPC (redrawn from Fig. 7 of Tank et al., 1982). Observed values of D are given in μm^2/s; calculated values are normalized to one at $c \rightarrow 0$.

There are several possible explanations for the discrepancy.

(*a*) The effect of boundary lipids. To examine their effect, we assume that a complete shell of 30 lipids (Heyn et al., 1981) is rigidly bound to BR and recalculate the diffusion constants, using $a_P = [8.75 + 30(0.657)]$ nm^2 in Eq. 13; these results are also shown in Fig. 6 *a*. Even this extreme assumption does not decrease the diffusion constant enough to match the observed values for BR. In ROS, ~38% of the lipids are motionally restricted as shown by electron spin resonance (Watts, 1982). If these lipids were rigidly bound to rhodopsin, Eq. 12 would give $D^* = 0.42$. This value is still somewhat greater than the measured values.

(*b*) Association of protein. Rotational diffusion measurements show that BR begins to form clusters at a lipid/protein molar ratio of 100:1 (Cherry and Godfrey, 1981), corresponding to a protein area fraction of 0.12. But formation of the trimer will have little effect on the observed diffusion constant. The equation of Saffman and Delbrück (1975) shows that at infinite dilution the diffusion constant of trimer is ~10% lower than that of monomer. Fig. 5 shows that the effect of concentration on the diffusion constant for hexagons of radius 1–4 is independent of radius. So it should not make much difference whether a given area fraction of BR is present as monomer

or as trimer. This conclusion agrees with the experimental results of Vaz and co-workers on various proteins (Clegg and Vaz, 1985).

(c) Protein–protein interactions. Diffusion rates can be affected by hydrodynamic interactions, a lipid-mediated interaction, or a protein–protein potential. The theoretical results of Ohtsuki and Okano (1982) for interacting Brownian particles in three dimensions suggest that any protein–protein potential, attractive or repulsive, will reduce the diffusion constant for self-diffusion (see also Abney et al., 1987). But note that for BR, Pearson et al. (1983) found that they could simulate the observed pair distribution function using only a hard-core repulsion.

(d) Perturbation of the lipid viscosity by the protein. This has been suggested frequently (see, for example, Jacobson et al., 1981; Cherry and Godfrey, 1981; Peters and Cherry, 1982), but up to now there has been no way to separate the effect of the protein as an obstacle from its effect on lipid dynamics.

Lipid Diffusion in the Presence of Protein. Tank et al. (1982a) and Peters and Cherry (1982) also measured diffusion constants of lipid analogues as a function of protein concentration. Their results are shown in Fig. 7.

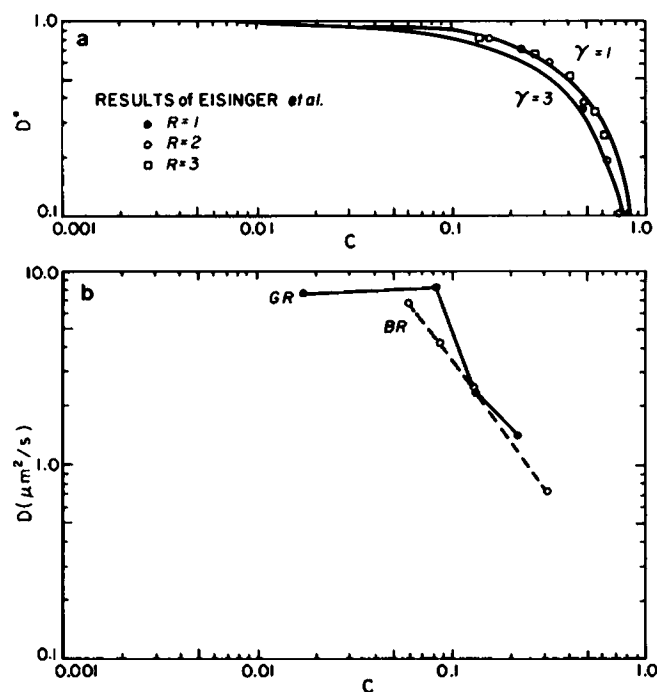Strictly speaking, to describe these experiments in terms

FIGURE 7 Lateral diffusion constants for lipids as a function of the area fraction of protein. (a) Calculated values for mobile point obstacles from Eqs 4–6 for $\gamma - 1$ and 3, and for immobile hexagonal obstacles (from Table II of Eisinger et al., 1986 for D as a function of f_{LP}). (b) Observed values for diO-C$_{18}$[3] in bacteriorhodopsin-DMPC mixtures (from Table 3 of Peters and Cherry, 1982) and NBD-PE in gramicidin-DMPC mixtures (redrawn from Fig. 7 of Tank et al., 1982). Observed values of D are given in μm^2/s; calculated values are normalized to one.

of the Monte Carlo calculations, we would need values of the diffusion constant for point tracers in the presence of mobile hexagonal obstacles. These are not yet available, but Eqs. 4–6 give values for point tracers in the presence of mobile point obstacles, and the calculations of Eisinger et al. (1986) give values for point tracers in the presence of immobile hexagonal obstacles. As shown in Fig. 7, the two treatments give similar values of $D^*(c)$.

To apply Eqs. 4–6, we need a value of γ (Eq. 7). If we use the observed values of D at the lowest protein concentrations, we obtain $\gamma_{BR} = 2.0$ and $\gamma_{GR} = 2.1$. (One could also use Eqs. 4–6 to extrapolate those values of D to zero concentration; this would change the γ's by a few percent.) In Fig. 7, curves for $\gamma = 1$ and $\gamma = 3$ are plotted to show the sensitivity of D to γ.

Again, the observed decrease in D^* is greater than the calculated value. Possible causes include: (a) Perturbation of the lipid viscosity by the protein. (b) Protein–lipid interactions; in particular, an attraction leading to transient binding of the lipid analogue to protein. If the probe is preferentially bound to the protein, the lipid diffusion constant will be decreased (Elson and Reidler, 1979; Jacobson et al., 1981; Jähnig, 1981; Koppel et al., 1981).

DISCUSSION

These results on lipids and proteins indicate that the geometrical effects modeled in this paper have a significant effect on the diffusion constants of both lipids and proteins, but are not sufficient to account for the entire concentration effect observed. The diffusion constants of both lipids and proteins are lower than the calculated values, suggesting that the dominant factor is an increase in lipid viscosity due to the proteins.

Blebs and spherocytes could be a particularly favorable case for a test of protein effects on lipid diffusion. Neither the perturbation of lipid viscosity by proteins nor the transient binding of probe to protein is likely to depend on the attachment of the proteins to the cytoskeleton. To a first approximation, the only difference between native and perturbed membrane is the mobility of the obstacles (provided, of course, that the compositions of the native and perturbed membranes are the same).

The effect of protein–protein interaction can be examined in various ways. Monte Carlo calculations can be carried out for interacting particles; a simple case of this was recently treated by Pink et al. (1986). Distribution functions of proteins in membranes can be obtained from electron micrographs and used to test models of the protein–protein interaction (Pearson et al., 1983) and to calculate an effective pair potential (Braun et al., 1984). This potential can then be used to calculate the diffusion constant (Abney et al., 1987).

It would be helpful if two points were considered in designing experiments on diffusion in the presence of obstacles. First, the theory gives values of the diffusion constant relative to the limiting value at zero concentration

of protein, so that measurements at two or three low values of c would be useful. Second, the current form of the theory assumes randomly distributed obstacles and cannot be applied to systems in which the proteins form large clusters. The use of a nonaggregating protein would permit a larger range of protein concentrations to be used.

In summary, the theory of Tahir-Kheli (1983) and of Van Beijeren and Kutner (1985) allows us to treat the "archipelago effect"—the obstruction of diffusion by immobile species—and the concentration dependence of lateral diffusion of proteins in a unified manner, and allows calculation of D^* for arbitrary ratios of the jump rate of obstacles to the jump rate of tracers. The Monte Carlo model presented predicts the geometrical effect of obstacles on diffusion, making it possible to separate purely geometrical effects from those of protein–protein and protein–lipid interactions. The geometrical effects and the sum of the other effects appear to be of comparable magnitude.

REFERENCES

Abney, J. R., B. A. Scalettar, and J. C. Owicki. 1987. Concentration and time dependent self-diffusion of interacting membrane proteins. *Biophys. J.* 51 (2, Pt. 2):541a. (Abstr.)

Axelrod, D. 1983. Lateral motion of membrane proteins and biological function. *J. Membr. Biol.* 75:1–10.

Braun, J., J. R. Abney, and J. C. Owicki. 1984. How a gap junction maintains its structure. *Nature (Lond.).* 310:316–318.

Chazotte, B., E.-S. Wu, and C. R. Hackenbrock. 1984. Effect of varied membrane protein density on the lateral diffusion of lipids in the mitochondrial inner membrane. *Biochem. Soc. Trans.* 12:463–464.

Cherry, R. J., and R. E. Godfrey. 1981. Anisotropic rotation of bacteriorhodopsin in lipid membranes. *Biophys. J.* 36:257–276.

Clegg, R. M., and W. L. C. Vaz. 1985. Translational diffusion of proteins and lipids in artificial lipid bilayer membranes. A comparison of experiment with theory. *In* Progress in Protein-Lipid Interactions. A. Watts and J. J. H. H. M. DePont, editors. Elsevier North-Holland Biomedical Press, Amsterdam. 173–229.

Dratz, E. A., and P. A. Hargrave. 1983. The structure of rhodopsin and the rod outer segment disk membrane. *Trends Biochem. Sci.* 8:128–131.

Eisinger, J., J. Flores, and W. P. Petersen. 1986. A milling crowd model for local and long-range obstructed lateral diffusion. *Biophys. J.* 49:987–1001.

Elson, E. L., and J. A. Reidler. 1979. Analysis of cell surface interactions by measurements of lateral mobility. *J. Supramol. Struct.* 12:481–489.

Galla, H.-J., W. Hartmann, U. Theilen, and E. Sackmann. 1979. On two-dimensional passive random walk in lipid bilayers and fluid pathways in biomembranes. *J. Membr. Biol.* 48:215–236.

Gebele, T. 1984. Site percolation threshold for square lattice. *J. Phys. A.* 17:L51–L54.

Heyn, M. P., A. Blume, M. Rehorek, and N. A. Dencher. 1981. Calorimetric and fluorescence depolarization studies on the lipid phase transition of bacteriorhodopsin-dimyristoylphosphatidylcholine vesicles. *Biochemistry.* 20:7109–7115.

Henderson, R., and P. N. T. Unwin. 1975. Three-dimensional model of purple membrane obtained by electron microscopy. *Nature (Lond.).* 257:28–32.

Hughes, B. D., B. A. Pailthorpe, L. R. White, and W. H. Sawyer. 1982. Extraction of membrane microviscosity from translational and rotational diffusion coefficients. *Biophys. J.* 37:673–676.

Jacobson, K., Y. Hou, Z. Derzko, J. Wojcieszyn, and D. Organisciak. 1981. Lipid lateral diffusion in the surface membrane of cells and in multibilayers formed from plasma membrane lipids. *Biochemistry.* 20:5268–5275.

Jähnig, F. 1981. No need for a new membrane model. *Nature (Lond.).* 289:694–696.

Kalle, C., and S. Wansleben. 1984. Problems with the random number generator RANF implemented on the CDC Cyber 205. *Comp. Phys. Comm.* 33:343–346.

Kehr, K. W., and K. Binder. 1984. Simulation of diffusion in lattice gases and related kinetic phenomena. *In* Applications of the Monte Carlo Method in Statistical Physics. K. Binder, editor. Springer-Verlag, Berlin. 181–221.

Kell, D. B. 1984. Constraints on the lateral diffusion of membrane proteins in prokaryotes. *Trends Biochem. Sci.* 9:379.

Kirkpatrick, S., and E. P. Stoll. 1981. A very fast shift-register sequence random number generator. *J. Comput. Phys.* 40:517–526.

Koppel, D. E., M. J. Osborn, and M. Schindler. 1981a. Reply (to comments of F. Jähnig). *Nature (Lond.).* 289:696.

Koppel, D. E., M. P. Sheetz, and M. Schindler. 1981b. Matrix control of protein diffusion in biological membranes. *Proc. Natl. Acad. Sci. USA.* 78:3576–3580.

Kutner, R., and K. W. Kehr. 1983. Diffusion in concentrated lattice gases. IV. Diffusion coefficient of tracer particle with different jump rate. *Phil. Mag.* A48:199–213.

Le Claire, A. D. 1970. Correlation effects in diffusion in solids. *In* Physical Chemistry. An Advanced Treatise. Vol. X. W. Jost, editor. 261–330.

Lewis, B. A., and D. M. Engelman. 1983. Lipid bilayer thickness varies linearly with acyl chain length in fluid phosphatidylcholine vesicles. *J. Mol. Biol.* 166:211–217.

Li, P., and W. Strieder. 1982. Monte Carlo simulation of the conductivity of the two-dimensional triangular site network. *J. Phys. Comm.* 15:6591–6595.

Liebman, P. A., and G. Entine. 1974. Lateral diffusion of visual pigment in photoreceptor disk membranes. *Science (Wash. DC).* 185:457–459.

MacCarthy, J. E., and J. J. Kozak. 1982. Lateral diffusion in fluid systems. *J. Chem. Phys.* 77:2214–2216.

McCloskey, M., and M.-M. Poo. 1984. Protein diffusion in cell membranes: some biological implications. *Int. Rev. Cytol.* 87:19–81.

Mitescu, C. D., and J. Roussenq. 1983. Diffusion on percolation clusters. *Ann. Israel Phys. Soc.* 5:81–100.

Ohtsuki, T., and K. Okano. 1982. Diffusion constants of interacting Brownian particles. *J. Chem. Phys.* 77:1443–1450.

Onoda, G. Y., and E. G. Liniger. 1986. Experimental determination of the random-parking limit in two dimensions. *Phys. Rev. A.* 33:715–716.

Pearson, L. T., S. I. Chan, B. A. Lewis, and D. M. Engelman. 1983. Pair distribution functions of bacteriorhodopsin and rhodopsin in model bilayers. *Biophys. J.* 43:167–174.

Peters, R., and R. J. Cherry. 1982. Lateral and rotational diffusion of bacteriorhodopsin in lipid bilayers: experimental test of the Saffman-Delbrück equations. *Proc. Natl. Acad. Sci. USA.* 79:4317–4321.

Pink, D. A. 1985. Protein lateral movement in lipid bilayers. Stimulation studies of its dependence upon protein concentration. *Biochim. Biophys. Acta.* 818:200–204.

Pink, D. A., D. J. Laidlaw, and D. M. Chisholm. 1986. Protein lateral

movement in lipid bilayers. Monte Carlo simulation studies of its dependence upon attractive protein-protein interactions. *Biochim. Biophys. Acta.* 863:9–17.

Poo, M.-M., and R. A. Cone. 1974. Lateral diffusion of rhodopsin in the photoreceptor membrane. *Nature (Lond.).* 247:438–441.

Saffman, P. G., and M. Delbrück. 1975. Brownian motion in biological membranes. *Proc. Natl. Acad. Sci. USA.* 72:3111–3113.

Saxton, M. J. 1982. Lateral diffusion in an archipelago: effects of impermeable patches on diffusion in a cell membrane. *Biophys. J.* 39:165–173.

Saxton, M. J. 1986. Lateral diffusion in an archipelago: the effect of mobile obstacles. *Biophys. J.* 49 (2, Pt. 2):311a. (Abstr.)

Schindler, M., M. J. Osborn, and D. E. Koppel. 1980. Lateral mobility in reconstituted membranes—comparisons with diffusion in polymers. *Nature (Lond.).* 283:346–350.

Schlessinger, J. 1980. The mechanism and role of hormone-induced clustering of membrane receptors. *Trends Biochem. Sci.* 5:210–214.

Sowers, A. E., and C. R. Hackenbrock. 1985. Variation in protein lateral diffusion coefficients is related to variation in protein concentration found in mitochondrial inner membranes. *Biochim. Biophys. Acta.* 821:85–90.

Stauffer, D. 1985. Introduction to percolation theory. Taylor & Francis, London and Philadelphia.

Straley, J. P. 1980. The ant in the labyrinth: diffusion in random networks near the percolation threshold. *J. Phys. C.* 13:2991–3002.

Tahir-Kheli, R. A. 1983. Correlation factors for atomic diffusion in nondilute multicomponent alloys with arbitrary vacancy concentration. *Phys. Rev. B.* 28:3049–3056.

Tahir-Kheli, R. A., and N. El-Meshad. 1985. Correlated diffusion in two-dimensional systems. *Phys. Rev. B.* 32:6166–6175.

Tank, D. W., E.-S. Wu, P. R. Meers, and W. W. Webb. 1982a. Lateral diffusion of gramicidin C in phospholipid multibilayers. *Biophys. J.* 40:129–135.

Tank, D. W., E.-S. Wu, and W. W. Webb. 1982b. Enhanced molecular diffusibility in muscle membrane blebs: release of lateral constraints. *J. Cell Biol.* 92:207–212.

Van Beijeren, H., and R. Kutner. 1985. Mean square displacement of a tracer particle in a hard-core lattice gas. *Phys. Rev. Lett.* 55:238–241.

Vaz, W. L. C., M. Criado, V. M. C. Madeira, G. Schoellmann, and T. M. Jovin. 1982. Size dependence of the translational diffusion of large integral membrane proteins in liquid-crystalline phase lipid bilayers. A study using fluorescence recovery after photobleaching. *Biochemistry.* 21:5608–5612.

Vaz, W. L. C., F. Goodsaid-Zalduondo, and K. Jacobson. 1984. Lateral diffusion of lipids and proteins in bilayer membranes. *FEBS (Fed. Eur. Biochem. Soc.) Lett.* 174:199–207.

Watts, A. 1982. Magnetic resonance studies of vertebrate rod outer segments. *Prog. Retinal Res.* 1:153–178.

Webb, W. W., L. S. Barak, D. W. Tank, and E.-S. Wu. 1981. Molecular mobility on the cell surface. *Biochem. Soc. Symp.* 46:191–205.

Wu, E.-S., D. W. Tank, and W. W. Webb. 1982. Unconstrained lateral diffusion of concanavalin A receptors on bulbous lymphocytes. *Proc. Natl. Acad. Sci. USA.* 79:4962–4966.